BIOCHEMISTRY
including biophysical chemistry & molecular biology

Article

pubs.acs.org/biochemistry

Biophysical Comparison of Soluble Amyloid-β(1−42) Protofibrils, Oligomers, and Protofilaments

Michael R. Nichols,* Benjamin A. Colvin, Elizabeth A. Hood, Geeta S. Paranjape, David C. Osborn, and Shana E. Terrill-Usery

Department of Chemistry and Biochemistry and Center for Nanoscience, University of Missouri—St. Louis, One University Boulevard, St. Louis, Missouri 63121, United States

ABSTRACT: Some of the pathological hallmarks of the Alzheimer's disease brain are senile plaques composed of insoluble amyloid-β protein (Aβ) fibrils. However, much of the recent emphasis in research has been on soluble Aβ aggregates in response to a growing body of evidence that shows that these species may be more neurotoxic than fibrils. Within this subset of soluble aggregated Aβ are protofibrils and oligomers. Although each species has been widely investigated separately, few studies have directly compared and contrasted their physical properties. In this work, we examined well-recognized preparations of Aβ(1−42) oligomers and protofibrils with multiangle (MALS) and dynamic (DLS) light scattering in line with, or following, size-exclusion chromatography (SEC). Multiple SEC−MALS analyses of protofibrils revealed molecular weight (M_w) gradients ranging from 200 to 2600 kDa. Oligomeric Aβ species are generally considered to be a smaller and more nascent than protofibrils. However, oligomer M_w values ranged from 225 to 3000 kDa, larger than that for protofibrils. Root-mean-square radius (R_g) values correlated with the M_w trends with protofibril R_g values ranging from 16 to 35 nm, while oligomers produced one population at 40−43 nm with a more disperse population from 22 to 39 nm. Hydrodynamic radius (R_H) measurements by DLS and thioflavin T fluorescence measurements indicated that protofibrils and oligomers had commonalities, yet electron microscopy revealed morphological differences between the two. SEC-purified Aβ(1−42) monomer at lower concentrations was slower to nucleate but formed protofibrils (1500 kDa) or soluble protofilaments (3000 kDa) depending on the buffer type. The findings from these studies shed new light on the similarities and differences between distinct soluble aggregated Aβ species.

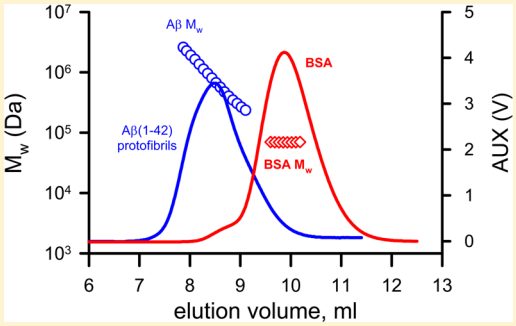

Alzheimer's disease (AD) is a progressive neurodegenerative illness diagnosed clinically by dementia and pathologically by the presence of neuritic plaques in the brain parenchyma and intracellular neurofibrillary tangles.[1] Accumulation of aggregated amyloid-β peptide (Aβ), the main component of the neuritic plaques,[2] is a critical step in the onset of Alzheimer's disease (AD). Aβ is produced as a 40- or 42-residue peptide following proteolysis of the amyloid-β precursor protein[3] and circulates physiologically in the plasma and cerebrospinal fluid.

Convincing evidence of the role of Aβ in AD comes from genetic studies of families that exhibit early onset familial AD (FAD). These studies have identified a number of nucleotide mutations closely linked to AD[4,5] that either increase Aβ levels or increase the propensity for Aβ aggregation. Furthermore, many of the genetic mutations that cause FAD increase the ratio of Aβ(1−42) to Aβ(1−40). The two additional hydrophobic amino acid residues on Aβ(1−42) substantially increase the propensity for aggregation.[6] It has been shown that neuritic plaques consist overwhelmingly of Aβ(1−42)[7] and that Aβ(1−42) forms a greater variety of soluble aggregated species.[8] Both of these observations, along with other findings, support the critical detrimental role of Aβ(1−42) in AD pathogenesis.[9] In fact, the cerebrospinal fluid (CSF) Aβ(1−42) level is one component of an important biomarker test for AD patients that also includes CSF tau and amyloid imaging.[10]

Numerous *in vitro* studies have shown that unstructured Aβ monomer will undergo noncovalent self-assembly[6] to form a polydisperse mixture of soluble oligomers[8,11,12] and/or protofibrils[12−14] with high β-sheet content[15] and ultimately insoluble fibrils.[16] Aβ assembly occurs via a nucleation-dependent polymerization process.[17] The rate-limiting nucleation step is characterized by a lag phase followed by rapid polymerization and fibril formation. The duration of the lag phase and conformational pathway are variable even in homogeneous aqueous solutions and are sensitive to many conditions, including pH, ionic strength, temperature, and agitation.[13,18−20] A secondary nucleation process may also occur whereby fibril surfaces stimulate new oligomer formation, resulting in the coexistence of both fibrils and oligomers in the same solution.[21]

Although there remains significant discussion about the impact of soluble and fibrillar forms of Aβ, much of the recent emphasis and focus has been on soluble Aβ aggregates.[22,23]

Received: August 1, 2014
Revised: March 5, 2015
Published: March 10, 2015

DOI: 10.1021/bi500957g
Biochemistry 2015, 54, 2193−2204

Within this class of soluble aggregated species are oligomers and protofibrils. Numerous studies support the toxicity or biological activity of each species.[18,24−27] The preparation of either oligomeric[20] or protofibrillar[15,28] Aβ has been well-documented. These methodologies have been used separately in a variety of studies, but a direct comparison between oligomers and protofibrils has not yet been made.

Multiangle light scattering (MALS) has proven to be a valuable technique for evaluating the self-assembly of multiple amyloid-forming proteins, including Aβ,[19,29] prions,[30] and α-synuclein.[31] Size-exclusion chromatography (SEC) in line with MALS (SEC−MALS) allows separation of polydisperse protein solutions and concurrent size determination. We have previously utilized both oligomer- and protofibril-forming conditions to prepare pools of proinflammatory Aβ for studies of microglial activation.[32] In this study, we utilized light scattering in conjunction with dye binding and microscopy to directly compare the biophysical features of those, as well as other, soluble Aβ(1−42) species.

EXPERIMENTAL PROCEDURES

Preparation of Aβ Peptides. Aβ(1−42) was obtained from the W. M. Keck Biotechnology Resource Laboratory (Yale School of Medicine, New Haven, CT) in lyophilized form and stored at −20 °C. Aβ peptide was dissolved in 100% hexafluoroisopropanol (HFIP) (Sigma-Aldrich, St. Louis, MO) to yield a 1 mM Aβ solution, separated into aliquots in sterile microcentrifuge tubes, and evaporated uncovered at room temperature overnight in a fume hood. The following day, the aliquots were vacuum-centrifuged to remove any residual HFIP and stored in desiccant at −20 °C. Aβ(1−42) protofibrils were prepared as previously described[32] by dissolving lyophilized Aβ (1 mg) in 50 mM NaOH to yield a 2.5 mM Aβ solution. The solution was then diluted to 250 μM Aβ in prefiltered (0.22 μm) artificial cerebrospinal fluid [aCSF, 15 mM $NaHCO_3$, 1 mM Na_2HPO_4, 130 mM NaCl, and 3 mM KCl (pH 7.8)]. Aβ(1−42) oligomers were prepared using a slightly modified version of the method of Stine et al.[20] in which lyophilized Aβ (1 mg) was dissolved in 100% dimethyl sulfoxide (DMSO) to yield a 5 mM Aβ solution. The solution was then diluted to 100 μM Aβ in prefiltered (0.22 μm) aCSF. The oligomer preparation was incubated for 24 h at 4 °C. Both preparations were centrifuged at 18000*g* for 10 min with a Beckman-Coulter Microfuge 18 instrument, prior to chromatographic analysis of the supernatants. To discourage protofibril or oligomer formation and increase monomer yields, aliquots of Aβ(1−42) were reconstituted in 6 M guanidine hydrochloride (GuHCl) and 10 mM NH_4OH, centrifuged, and eluted in the selected mobile phase.

Size-Exclusion Chromatography. Supernatants of Aβ(1−42) protofibrils and oligomers were fractionated in line with multiangle light scattering on a Superdex 75 HR 10/30 column (GE Healthcare) using an AKTA FPLC system (GE Healthcare). Prior to injection of Aβ, the Superdex 75 column was coated with 2 mg of bovine serum albumin (BSA) taken from a sterile 7.5% fraction V solution (Sigma) to prevent any nonspecific binding of Aβ to the column matrix. Following loading of the sample, Aβ was eluted at a rate of 0.5 mL min^{-1} in aCSF, and 0.5 mL fractions were collected and immediately placed on ice. In some cases, Aβ was eluted in 50 mM tris(hydroxymethyl)aminomethane hydrochloride (Tris-HCl) (pH 7.8) or aCSF containing 30 mM NaCl (pH 7.8) (aCSF low NaCl). Aβ concentrations were determined by in-line UV absorbance using an extinction coefficient of 1450 cm^{-1} M^{-1} at 280 nm. A higher-purity (≥97%) lyophilized BSA monomer was utilized for molecular weight determination (Sigma). In some cases, Aβ(1−42) monomers were purified by SEC prior to aggregation assays to remove any preexisting aggregates. The elution conditions were the same as those described above, and monomers were recovered in the selected SEC mobile phase. For aggregation assays using SEC-purified monomers, samples were incubated in siliconized tubes at either 37 °C in a water bath using a flotation pad, 20 °C on the benchtop, or 4 °C in the refrigerator.

Multiangle Light Scattering (MALS). MALS data were obtained in line with SEC using a DAWN DSP instrument (Wyatt Technology, Santa Barbara, CA). Samples were analyzed under continuous flow through a K12 quartz cell and illuminated with a helium−neon laser. Light scattering data were obtained every 0.167 mL at fixed-angle detectors 4−16 and plotted using the Debye formalism of the Rayleigh−Debye−Gans approximation[33,34] for large anisotropic particles (eq 1).

$$R_\theta/Kc = M_w P(\theta) \quad (1)$$

This equation relates the Rayleigh ratio (scattering intensity) to molecular weight (M_w) multiplied by a form factor, $P(\theta)$, where c is the solute concentration (grams per milliliter), θ is the scattering angle, K is an optical constant equal to $4\pi^2(dn/dc)^2 n_o^2 \lambda_o^{-4} N_A^{-1}$, n is the refractive index of the solution, n_o is the refractive index of the solvent, λ_o is the wavelength of incident light in a vacuum (632.8 nm), and N_A is Avogadro's number. $P(\theta)$, which takes into account the destructive interference of scattering by large particles, is the scattering intensity for a large particle divided by the scattering intensity without interference and can be expanded in a power series. The limiting form of the form factor equation as θ approaches zero is shown in eq 2, where R_g^2 is the mean square radius and λ is λ_o/n_o.

$$P(\theta) = 1 - (16\pi^2/3\lambda^2) R_g^2 \sin^2(\theta/2) \quad (2)$$

Substitution of eq 2 into eq 1 and plotting R_θ/Kc versus $\sin^2(\theta/2)$ yield M_w as the y-intercept and a limiting slope equal to $M_w(16\pi^2/3\lambda^2)R_g^2$. Debye plots were fit with a linear regression using dn/dc values for Aβ and BSA of 0.186 and 0.190 mL/g, respectively.

Dynamic Light Scattering. Hydrodynamic radius (R_H) measurements were taken at room temperature with a DynaPro Titan instrument (Wyatt Technology). Samples (35 μL) were placed directly into a quartz cuvette, and the light scattering intensity was collected at a 90° angle using a 5 s acquisition time. Particle diffusion coefficients were calculated from autocorrelated light intensity data (>25 acquisitions) and converted to R_H with the Stokes−Einstein equation. Mean R_H values were obtained with Dynamics software (version 6.12.03). Histograms were generated by Dynamics data regularization, and intensity-weighted or mass-weighted mean R_H values were derived from the regularized histograms of either percent intensity or mass versus R_H, respectively.

Thioflavin T Fluorescence. Aβ solutions were assessed by ThT fluorescence as described previously.[19] Aβ aliquots were diluted to 5 μM in aCSF pH 7.8 containing 5 μM ThT. Fluorescence emission scans (460−520 nm) were conducted on a Cary Eclipse fluorescence spectrophotometer using an excitation wavelength of 450 nm and integrated from 470 to

DOI: 10.1021/bi500957g
Biochemistry 2015, 54, 2193−2204

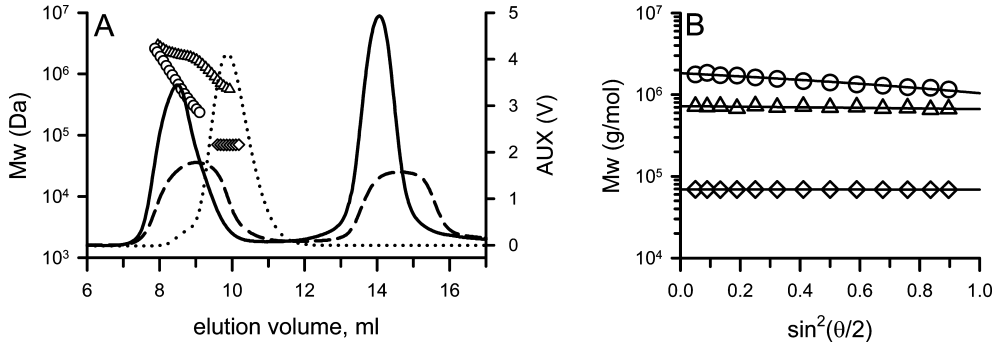

Figure 1. Molecular weight comparison using SEC−MALS. (A) Aβ(1−42) protofibrils and oligomers prepared as described in Experimental Procedures and purified BSA were characterized by SEC−MALS. The absorbance at 280 nm was monitored in line with SEC and converted to voltage (V) using an auxiliary constant calculated for each species. The absorbance-determined concentration traces (right *y*-axis) are shown for Aβ(1−42) protofibrils (—), Aβ(1−42) oligomers (− − −), and BSA (···), which eluted between 7 and 12 mL. Aβ(1−42) monomers eluted between 13 and 16 mL. M_w values were obtained from Debye plots of MALS data taken from each slice (0.167 mL). The calculated M_w values (left *y*-axis) are plotted for Aβ(1−42) protofibrils (○), Aβ(1−42) oligomers (△), and BSA (◇). For the M_w plots, every fifth slice is shown for the sake of clarity and distinction between points. (B) Debye plots of the peak slices from panel A for Aβ(1−42) protofibrils (○), Aβ(1−42) oligomers (△), and BSA (◇) at 8.48, 9.00, and 9.87 mL, respectively.

500 nm to obtain ThT relative fluorescence values. Buffer controls did not show any significant ThT fluorescence in the absence of Aβ. All ThT fluorescence values are reported in relative fluorescence units.

Electron Microscopy. SEC-purified Aβ(1−42) protofibrils (10 μL) were applied to a 200-mesh Formvar-coated copper grid (Ted Pella, Inc.). Samples were allowed to adsorb for 10 min at 20 °C, followed by removal of excess sample solution. Grids were washed three times by placing them sample side down on a droplet of water. Heavy metal staining was conducted by incubation of the grid on a droplet of 2% uranyl acetate (Electron Microscopy Sciences, Hatfield, PA) for 10 min, removal of excess solution, and air drying. Affixed samples were visualized with a JEOL JEM-2000 FX transmission electron microscope operated at 200K eV.

Circular Dichroism. Samples (0.2 mL) were placed into a rectangular quartz cuvette with a 0.1 cm path length, or smaller volumes (15 μL) were measured via a quartz-windowed microsampling disc (Jasco) with a 0.1 cm path length. Spectra were obtained by wavelength scan from 260 to 190 nm using a Jasco J-1500 circular dichroism spectrometer, and four successive wavelength scans were averaged for each Aβ sample. Buffer control spectra were averaged and subtracted from Aβ sample spectra, and each resulting point ($[\theta]_{obs}$, degrees) was converted to mean residue ellipticity ($[\theta]$, degrees square centimeter per decimole) with the equation $[\theta] = [\theta]_{obs}(MRW/10lc)$, where MRW is the mean residue molecular weight of Aβ(1−42) (4514.1 g/mol divided by 42 residues), l is the optical path length (centimeters), and c is the concentration (grams per cubic centimeter). Secondary structure estimates were obtained using the modified Contin method (CONTINLL) available through the CDPro suite of analysis programs.[35] The SMP56 protein reference set was used to estimate percentages of Aβ(1−42) secondary structure from unsmoothed data over the range of 260−196 nm.

RESULTS

Multiangle Light Scattering Analysis of Aβ Protofibrils and Oligomers. Equivalent aliquots (1 mg) of HFIP-treated and lyophilized dry Aβ(1−42) were brought into solution separately using previously reported protofibril-forming[14,28,32] and oligomer-forming[20] procedures and conditions (described in Experimental Procedures). Rather than phenol red-free F-12 cell culture medium, the Aβ species were allowed to form in aCSF. We have recently described Aβ protofibril formation in aCSF,[36] a carbonate/phosphate buffering system (pH 7.8) similar in composition to phenol red-free F-12, but without glucose, Ca^{2+}, and Mg^{2+}. For protofibrils, the solution (1 mL) was centrifuged immediately, without additional incubation time, at 18000*g* for 10 min and the supernatant characterized by SEC−MALS. Elution of the Aβ(1−42) protofibril solution on Superdex 75 yielded a distinct two-population separation of protofibrils and monomers as monitored by 280 nm absorbance (Figure 1A, solid line). Light scattering data were collected continuously during the elution at 13 fixed angles and analyzed in 0.0167 mL data fractions or "slices". Each slice was analyzed with a Debye plot shown in Figure 1B. A linear fit of the angle-dependent light scattering intensity for each elution slice allowed the determination of M_w from the *y*-intercept and root-mean-square radius (R_g) from the slope. M_w values taken from the full width at half-maximum of the protofibril concentration peak (7.87−9.13 mL) ranged from 2600 kDa (576 monomers) at the leading side to 228 kDa (50 monomers) for the trailing side (Figure 1, circles). Although the protofibril fraction eluted in the void volume, a significant degree of size separation was observed. This is the first SEC−MALS analysis of this frequently reported method of protofibril preparation, and a large degree of size polydispersity was evident rather than a homogeneous population of similarly sized aggregates. The pattern of protofibril elution was a smooth decreasing gradient of sizes with an even distribution of M_w values across the protofibril peak. For validation purposes, SEC−MALS was used to characterize a purified BSA/aCSF solution. BSA (Figure 1, dotted line) eluted in the included volume of the Superdex 75 column (fractionation range of 3−70 kDa), and the measured mean BSA M_w ± standard deviation (SD) from 44 slices (Figure 1, diamonds) across the concentration peak was 69.6 ± 0.6 kDa.

We also utilized a commonly used and well-described method for preparing oligomeric Aβ, which entails reconstitution of the dry Aβ(1−42) peptide in DMSO followed by dilution into cold F12 medium and incubation for 24 h at 4 °C.[20] For this investigation, phenol red-free F-12 medium was replaced with aCSF.[36] The same SEC−MALS analysis was

DOI: 10.1021/bi500957g
Biochemistry 2015, 54, 2193−2204

conducted on an Aβ(1−42) oligomer preparation. Because oligomers are formed at 100 μM rather than 250 μM for the protofibrils, twice the volume was loaded onto the column so that total amounts of Aβ were closer to equivalent. The oligomers began to elute at the same time as the protofibrils, but the larger injection volume resulted in some peak broadening. The oligomer elution also displayed two major populations (monomers and higher-molecular weight species) with no evidence of intermediate species between the two peaks. The M_w range for Aβ(1−42) oligomers taken from the full width at half-maximum of the void volume concentration peak (7.95−9.93 mL) ranged from 2967 kDa (657 monomers) at the leading edge of the concentration peak to 588 kDa (130 monomers) at the trailing side edge of the concentration peak (Figure 1, triangles). Debye plots of slices taken from the protofibril, oligomer, and BSA concentration peaks in Figure 1A are shown in Figure 1B and represent the largest population of each protein eluted from the column. M_w values determined from the three plots were 69 kDa for BSA, 723 kDa for Aβ(1−42) protofibrils, and 1718 kDa for Aβ(1−42) oligomers.

R_g is a size parameter based on the center of mass and internal distribution of individual mass elements for a particular particle. z-average R_g values were obtained from the same protofibril and oligomer SEC−MALS elutions shown in Figure 1, and these values corresponded directly with the M_w measurements in each slice. In Figure 2, the 90° detector

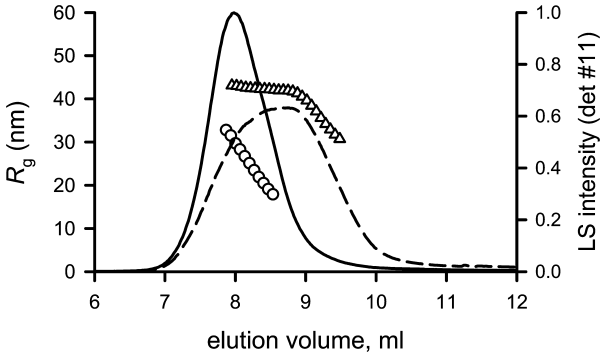

Figure 2. In-line R_g determination of Aβ(1−42) preparations. R_g values were obtained from Debye plots constructed during the SEC−MALS analysis in Figure 1. The light scattering intensity (right y-axis) from the 90° detector (detector 11) during the elution is shown for Aβ(1−42) protofibrils (—) and oligomers (– – –). R_g values plotted above (left y-axis) represent 50% of the maximal concentration trace for the leading edge to 50% of the maximal light scattering intensity trace for the trailing edge.

light scattering trace is shown rather than the concentration trace. Values of R_g for Aβ(1−42) protofibrils were much smaller than those of the Aβ(1−42) oligomers. Protofibrils ranged from 33 nm (leading edge) to 18 nm (trailing edge) (z-averaged mean of 25 nm), while oligomers displayed a more homogeneous population from 40 to 43 nm before decreasing in size from 40 to 30 nm across the trailing side of the light scattering peak (z-averaged mean of 40 nm) (Figure 2).

A second SEC−MALS analysis was conducted in which the protofibril and oligomer preparations were analyzed on the same day in successive SEC−MALS runs. This set of experiments revealed that protofibril preparations were very reproducible. Identical aggregation conditions produced similar protofibril M_w distributions (Figure 3) ranging from 2418000 Da (leading edge) to 296600 Da (trailing edge). Oligomer

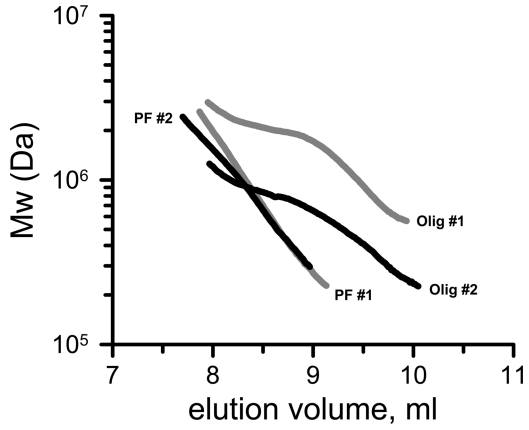

Figure 3. Protofibril preparation yields a consistent M_w range, while the oligomer preparation is more variable. Aβ(1−42) protofibrils and oligomers (each 1 mg dry weight) were prepared as described in Experimental Procedures and the legend of Figure 1. The oligomer preparation was initiated the previous day to allow successive SEC−MALS analyses to be conducted. The in-line SEC−MALS-determined M_w range during elution is shown for the first preparation of protofibrils (PF #1, gray line) and oligomers (Olig #1, gray line) described in Figure 1. The M_w ranges obtained during the repeat experiment are shown as black lines for protofibrils (PF #2) and oligomers (Olig #2).

sizes, however, were much more variable between preparations, and overall M_w values for the second preparation differed quite a bit from those of the first preparation (Figure 3). The oligomer M_w range in the second preparation was 1255 kDa (278 monomers) at the leading edge and 226 kDa (50 monomers) at the trailing edge. The variability in the M_w values between different oligomer preparations may be explained by the variability in nucleation lag time during the 24 h incubation time utilized for their formation. Protofibrils, on the other hand, are formed rapidly at the higher concentration under conditions outlined in Experimental Procedures, leaving less variability in lag time. Despite the differences in oligomer M_w between preparations, R_g values for the second protofibril and oligomer preparations were similar to those of the initial preparations. Aβ(1−42) protofibrils ranged from 31 to 17 nm across the light scattering peak (z-averaged mean of 25 nm) (Figure 4), while Aβ(1−42) oligomers ranged from 41 to 22 nm (z-averaged mean of 35 nm).

Dynamic Light Scattering Analysis. During the second round of analysis, dynamic light scattering (DLS) measurements of the collected fractions were included to obtain further information about the protofibril and oligomer preparations. Although the oligomers displayed rms radius values somewhat larger than those of protofibrils, the mean regularized hydrodynamic radius (R_H) obtained from intensity-weighted histograms for the oligomers (Figure 4, triangles) was similar to, but slightly lower than, that of the protofibrils (Figure 4, circles). R_H values for three fractions across the protofibril peak were 34 nm (8.0 mL), 30 nm (8.5 mL), and 22 nm (9.0 mL), while fractions across the oligomer peak were 31 nm (8.5 mL), 26 nm (9.0 mL), and 19 nm (9.5 mL). Averaging of the fraction R_H through the peak for protofibrils and oligomers yielded values of 29 and 25 nm, respectively. The unregularized mean R_H typically contains contributions from multiple particle populations, including trace amounts of very large particles and the buffer (solvent) component. The use of regularized histograms allows separation of particle populations and a

DOI: 10.1021/bi500957g
Biochemistry 2015, 54, 2193−2204

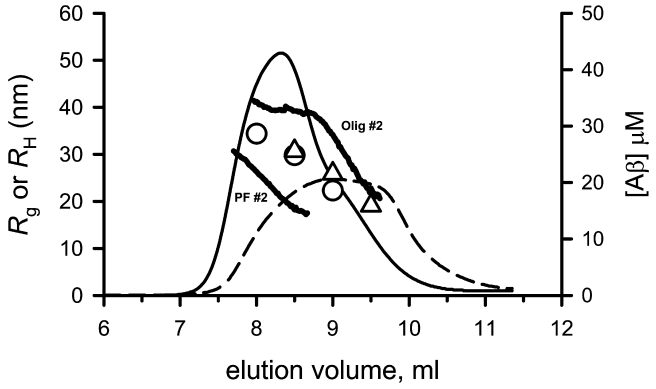

Figure 4. Comparison of R_g and R_H for Aβ(1−42) protofibrils and oligomers. R_g values were obtained in line during the second SEC−MALS analysis described in Figure 3. A UV absorbance trace was used to determine the Aβ concentration in line (right *y*-axis) for protofibrils (—) and oligomers (−−−). R_g values (left *y*-axis) are shown from 50% of the maximal concentration trace for the leading edge to 50% of the maximal light scattering intensity trace for the trailing edge for protofibrils (PF #2) and oligomers (Olig #2). R_H values (left *y*-axis) were determined in the fractions collected (#17, 8.0 mL; #18, 8.5 mL; #19, 9.0 mL; #20, 9.5 mL) during elution of the protofibrils (○) and oligomers (△).

better determination of Aβ protofibril or oligomer size. Particles that were detected by the instrument with an R_H of >1000 nm were not considered. R_H (DLS) was larger than R_g (MALS) for protofibrils but smaller for the oligomers in this particular experiment, but that was not the norm. The ratio between the two parameters can signify a particular conformation for a particle and is discussed in more detail below. In all, multiple preparations of Aβ(1−42) protofibrils (n = 4) and oligomers (n = 3) were analyzed, and the summary of the light scattering data is shown in Table 1. Although both Aβ preparations are polydisperse with respect to size, mean measurements were obtained over the multiple analyses and presented with the standard deviation between the analyses in Table 1. Overall, M_w, R_g, and R_H values were smaller for protofibrils than for oligomers. The combination of light scattering techniques provided a clearer picture of protofibril and oligomer sizes and indicated that both species were soluble, but relatively large, and contained somewhere between 50 and 660 monomer units. Protofibrils were routinely smaller in size and had a molecular weight lower than that of oligomers when adhering to the preparation conditions described in this report.

Table 1. Mean Sizes for Aβ(1−42) Protofibrils and Oligomers[a]

sample	M_w ± SD	R_g ± SD	R_H ± SD
protofibrils	884 ± 302 (4)	25.5 ± 1.8 (4)	23.6 ± 6.3 (3)
oligomers	1317 ± 595 (3)	37.1 ± 2.5 (3)	31.3 ± 5.5 (3)

[a]Values obtained from the full width at half-maximum of the concentration peak (n experiments). Units of kilodaltons for M_w and nanometers for R_g and R_H. R_H was determined from the regularized histogram of each fraction in the upper third of the SEC concentration peak and averaged together to yield an overall R_H for each protofibril or oligomer preparation.

Structure and Morphology Analysis. Thioflavin T (ThT) binding and fluorescence is a commonly used method for monitoring amyloid formation.[37] Dye binding and subsequent fluorescence emission at 482 nm correlate well with Aβ aggregation and formation of β-sheet secondary structure. While ThT has been used frequently to assess protofibrils, this is not typical with oligomer preparations. We have previously demonstrated that SEC-isolated Aβ(1−42) protofibrils exhibit significant ThT fluorescence, albeit much less than an equimolar solution of Aβ(1−42) fibrils, while SEC-isolated Aβ(1−42) monomers do not generate ThT fluorescence.[32,36] In this study, isolated Aβ(1−42) protofibrils and oligomers after SEC−MALS analysis were directly compared for ThT fluorescence. Fractions collected from a third SEC−MALS analysis of protofibrils and oligomers were assessed, and similar levels of ThT fluorescence were observed for all fractions through both protofibril and oligomer elution peaks (Figure 5). The final Aβ concentration was maintained at 5 μM in all fluorescence measurements. The ThT fluorescence findings indicated that oligomers contain elements of β-sheet and amyloid structure similar to that of protofibrils.

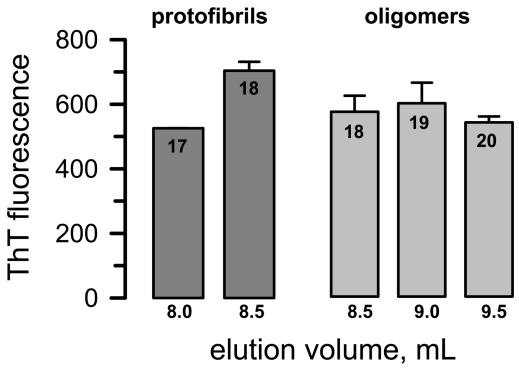

Figure 5. Aβ(1−42) protofibrils and oligomers have equivalent levels of thioflavin T binding and fluorescence. Aliquots of Aβ(1−42) protofibril and oligomer fractions collected after SEC−MALS analysis were diluted to 5 μM in aCSF containing 5 μM ThT, and fluorescence emission was measured and plotted as described in Experimental Procedures. Error bars represent the standard error of n = 3 ThT measurements. The numbers shown within the data bars indicate the collected fractions during elution and correspond to the fractions and elution volumes in the legend of Figure 4.

Morphological differences between isolated Aβ(1−42) protofibrils and oligomers were examined using transmission electron microscopy (TEM). We, and others, have previously used TEM to characterize Aβ(1−42) protofibrils.[14,32,38] Protofribrils are typically curvilinear structures <200 nm in length. High-magnification (59000×) TEM images of the protofibril fraction collected at 8.5 mL in Figure 3 revealed the classical morphology. Numerous small flexible Aβ(1−42) structures were observed (Figure 6A), and length analysis produced a mean value of 78 ± 35 nm (standard deviation). The analysis included only unambiguous protofibril structures and excluded the smaller species (<20 nm). The particular protofibril and oligomer fractions analyzed and depicted in the TEM image in Figure 6A were obtained following the SEC−MALS analysis presented in Figure 3 (PF #2, Olig #2). The corresponding M_w range for the protofibril fraction was 654−296 kDa with an average R_H of 30 nm. The oligomer fraction displayed none of the morphological characteristics of protofibrils despite possessing similar size features (M_w, 651−410 kDa; R_H, 26 nm). The Aβ(1−42) oligomers were globular spheroid shapes with a fair amount of polydispersity in cross-sectional distance (Figure 6B).

DOI: 10.1021/bi500957g
Biochemistry 2015, 54, 2193−2204

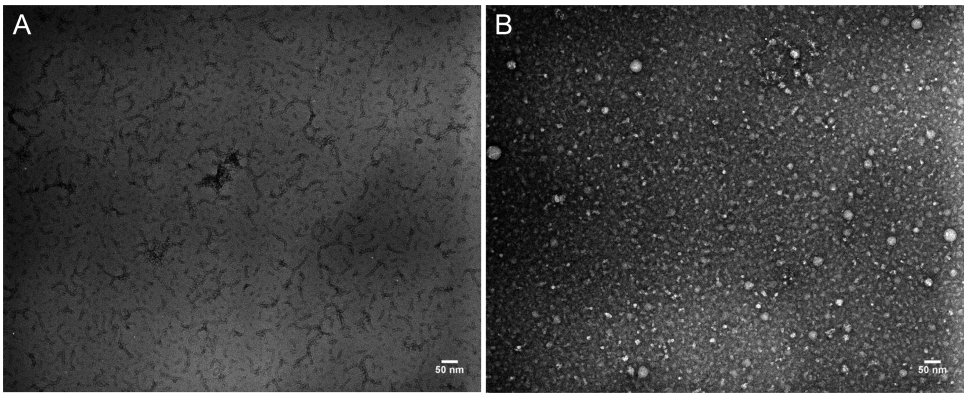

Figure 6. Morphological comparison between Aβ(1−42) protofibrils and oligomers. TEM images were obtained from the second Aβ(1−42) protofibril (A) and oligomer (B) preparation described in the legends of Figures 3 and 4. Samples were prepared as described from fractions collected after SEC−MALS analysis, and images were captured at 59000× magnification (scale bar of 50 nm). Length analysis was conducted manually utilizing the scale bar length to prepare 50, 100, and 150 nm increment bars to determine protofibril lengths in four quadrants of the image (total n = 106).

Analysis of Soluble Aβ(1−42) Species Formed from SEC-Purified Monomers. Every effort was made in the studies described above to precisely replicate the conventional protofibril and oligomer preparations from dry peptide films that have been reported in the literature. The results in this study indicate that high Aβ concentrations at room temperature favor rapid protofibril formation. However, working with stored dry Aβ(1−42) peptide samples without further purification may permit formation of preexisting structures that influence the ensuing aggregation process. For these studies, Aβ(1−42) was reconstituted in 6 M GuHCl containing 10 mM NH_4OH to suppress rapid protofibril formation and increase monomer yields. Monomer fractions were obtained from the Superdex 75 included volume, immediately placed on ice, and promptly used for aggregation studies. The Aβ(1−42) concentration of 40 μM was chosen so that 0.5 mL (90 μg Aβ) could be loaded for SEC−MALS and postelution evaluation. This amount was the realistic minimum for sample detection and analysis. SEC-purified monomeric Aβ(1−42) exhibited no ThT fluorescence (Figure 7A), and subsequent SEC repurification yielded no material in the Superdex 75 void volume (Figure 7B). SEC-purified Aβ(1−42) monomer incubated at 37 °C in aCSF demonstrated a lag phase of >4 h but then aggregated rapidly overnight (21 h). All of the ThT-fluorescent material was insoluble and was removed from the solution after centrifugation at 18000g for 10 min (Figure 7A). SEC analysis of the supernatant showed negligible material in the void volume and little remaining monomer in the included volume (Figure 7B), indicating a rapid progression from monomer to insoluble fibrils. Previous studies have shown a significant dependence on ionic strength for insoluble fibril formation.[19] Therefore, aCSF pH 7.8 was prepared with 30 mM NaCl, rather than 130 mM (aCSF low NaCl). Aβ(1−42) monomers purified by SEC in this buffer (40 μM) were incubated at 37 °C overnight and demonstrated a longer lag phase [>8 h (data not shown)] yet still progressed to a significant ThT fluorescence overnight (25 h); 90% of the ThT-positive Aβ(1−42) aggregates remained soluble after centrifugation (Figure 7A), and a substantial peak was observed in the SEC void volume (Figure 7B). Tris-HCl has frequently been used as a buffer for Aβ studies,[14,15,19] and it was employed in this study as a comparison to aCSF. Aβ(1−42) monomers purified via SEC in 50 mM Tris-HCl pH 7.8 (40 μM) were incubated at 37 °C overnight. The progression of aggregation for Aβ(1−42) in Tris-HCl was slightly slower than in aCSF low NaCl, yet a significantly lower percentage of the ThT-positive material (9%) remained soluble in the solution after centrifugation. SEC analysis matched this observation with less Aβ(1−42) overall eluted from the column.

Despite the loss of Aβ after centrifugation, a notable void volume peak was still present for evaluation. MALS analysis in line with SEC provided M_w and R_g values for the soluble Aβ(1−42) aggregates formed after a 37 °C incubation. M_w values for aggregates formed in aCSF low NaCl ranged from 3394 to 2961 kDa (mean of 3044 kDa, 674 monomers), while aggregates formed in Tris-HCl were notably smaller and ranged from 2133 to 1386 kDa (mean of 1533 kDa, 340 monomers) (Figure 7C). This observation was somewhat surprising in that much of the Aβ(1−42)/Tris-HCl solution was insoluble, which was indicative of fibril formation, yet the supernatant contained lower-M_w species. R_g values corresponded to the M_w determinations and ranged from 59 to 58 nm (mean of 59 nm) for aggregates formed in aCSF low NaCl and 43−37 nm (mean 39 nm) for aggregates formed in Tris-HCl (Figure 7D). DLS-generated R_H values for the postelution peak fractions were slightly harder to interpret because of polydispersity in the aCSF low NaCl aggregate solution. The percent intensity R_H, which can be skewed by larger species, was 139 nm, yet the largest percent mass population (83%) was found at 60 nm, similar to the R_g value (data not shown). R_H values for aggregates formed in Tris-HCl indicated less polydispersity with the greatest population based on the percent intensity at 25 nm and based on the percent mass at 17 nm (data not shown). The differences in morphology between the SEC-isolated Aβ(1−42) soluble aggregates formed in aCSF low NaCl pH 7.8 and 50 mM Tris-HCl pH 7.8 were quite striking. TEM images revealed long (>1 μm), slender protofilament structures in aCSF low NaCl (Figure 7E), while those in Tris-HCl were curvilinear protofibril structures 50−100 nm in length (Figure 7F). The observation of protofibrils in a Tris-HCl solution containing primarily insoluble fibrils demonstrated the coexistence of these two species prior to centrifugation and SEC isolation and emphasized the polydispersity that can occur in Aβ aggregation. The isolated Aβ(1−42) protofilaments from the aCSF low NaCl solution were fairly homogeneous with the peak SEC

DOI: 10.1021/bi500957g
Biochemistry 2015, 54, 2193−2204

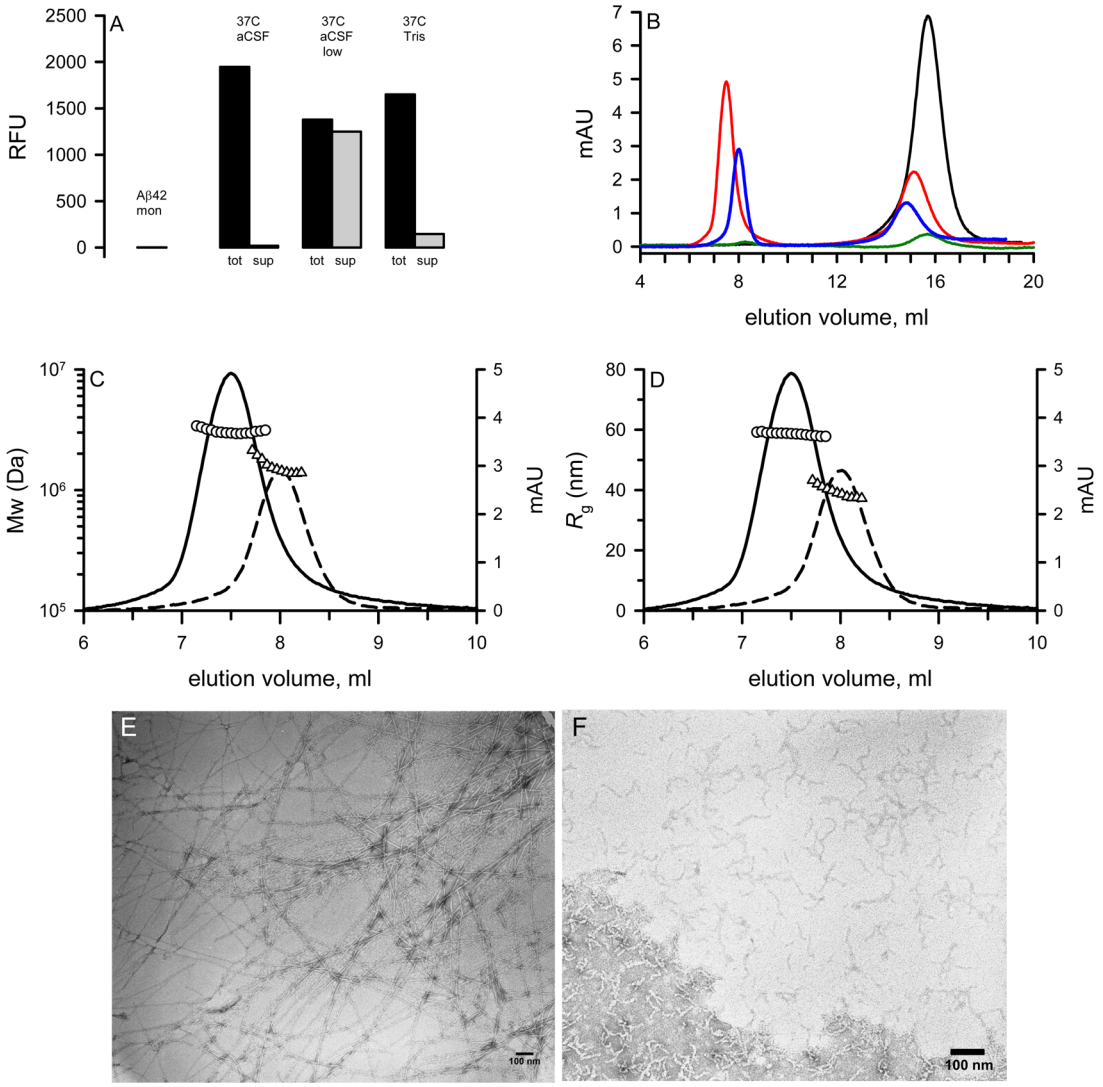

Figure 7. Ionic strength and buffer type influence soluble Aβ(1−42) aggregate formation by SEC-purified Aβ(1−42) monomers. (A) Following SEC purification of Aβ(1−42) monomers in differing buffers, ThT fluorescence measurements were taken at periodic times before (Aβ42 mon), during, and after incubation at 37 °C overnight. All solutions had an Aβ concentration of 40 μM. The final fluorescence time points are depicted in the plot and represent 21 h for monomers purified in aCSF pH 7.8, 25 h for monomers purified in aCSF low NaCl pH 7.8 (aCSF low), and 32 h for monomers purified in 50 mM Tris-HCl pH 7.8 (Tris). ThT fluorescence measurements were obtained from the solutions before (total), and in the supernatant (sup) after, centrifugation at 18000*g* for 10 min. At each time point and experimental step, ThT fluorescence was assessed in the absence of Aβ. These values ranged from 28 to 116 RFU and were subtracted from the Aβ/ThT values. (B) Supernatants (0.5 mL) from the solutions in panel A were repurified via SEC in their respective buffers, and the chromatograms obtained by 280 nm absorbance (mAU) are shown for Aβ(1−42) monomers in aCSF (black line) and the aCSF (green line), aCSF low NaCl (red line), and Tris (blue line) reactions. (C and D) SEC−MALS analysis was conducted on the soluble aggregates eluted in the Superdex 75 void volume. M_w (C) and R_g (D) values were determined every 0.167 mL for soluble Aβ(1−42) aggregates formed in aCSF low NaCl (○) and Tris (△). Every fourth value is shown for the sake of clarity and distinction between points. The 280 nm absorbance traces from panel B are reproduced for aCSF low NaCl (—) and Tris (−−−). (E and F) TEM images were obtained from the peak void volume fractions collected from the elutions shown in panels C and D. Images were captured at 35000× (E, aCSF low NaCl) and 59000× (F, Tris) magnifications (scale bars of 100 nm).

void volume fraction. Their preparation was quite reproducible as a second experiment produced similar long slender protofilament structures with a similar mean M_w and R_g (2896 kDa and 57 nm, respectively) (data not shown).

It was clear in our studies utilizing SEC-purified Aβ(1−42) monomers in aCSF low NaCl pH 7.8 that elongated, yet still quite soluble, protofilaments formed rapidly following nucleation. The rapid kinetics hindered observation of protofibrillar or oligomeric species. Because Aβ aggregation is temperature-dependent, additional incubations were conducted at 20 and 4 °C, and the aggregation kinetics were compared to those of the 37 °C incubation described above. Using ThT fluorescence as an aggregation marker, it was clear that nucleation of SEC-purified Aβ(1−42) monomers (40 μM) was keenly dependent on temperature, suggesting a significant activation energy barrier for aggregation initiation (Figure 8A). Following nucleation of the samples at the different temperatures, the solution supernatants after centrifugation were analyzed by ThT fluorescence and SEC. The 20 and 4 °C samples retained significant soluble ThT-positive material (92 and 68%, respectively) after centrifugation that was observed in the SEC void volume (Figure 8B). M_w and R_g values ranged

DOI: 10.1021/bi500957g
Biochemistry 2015, 54, 2193−2204

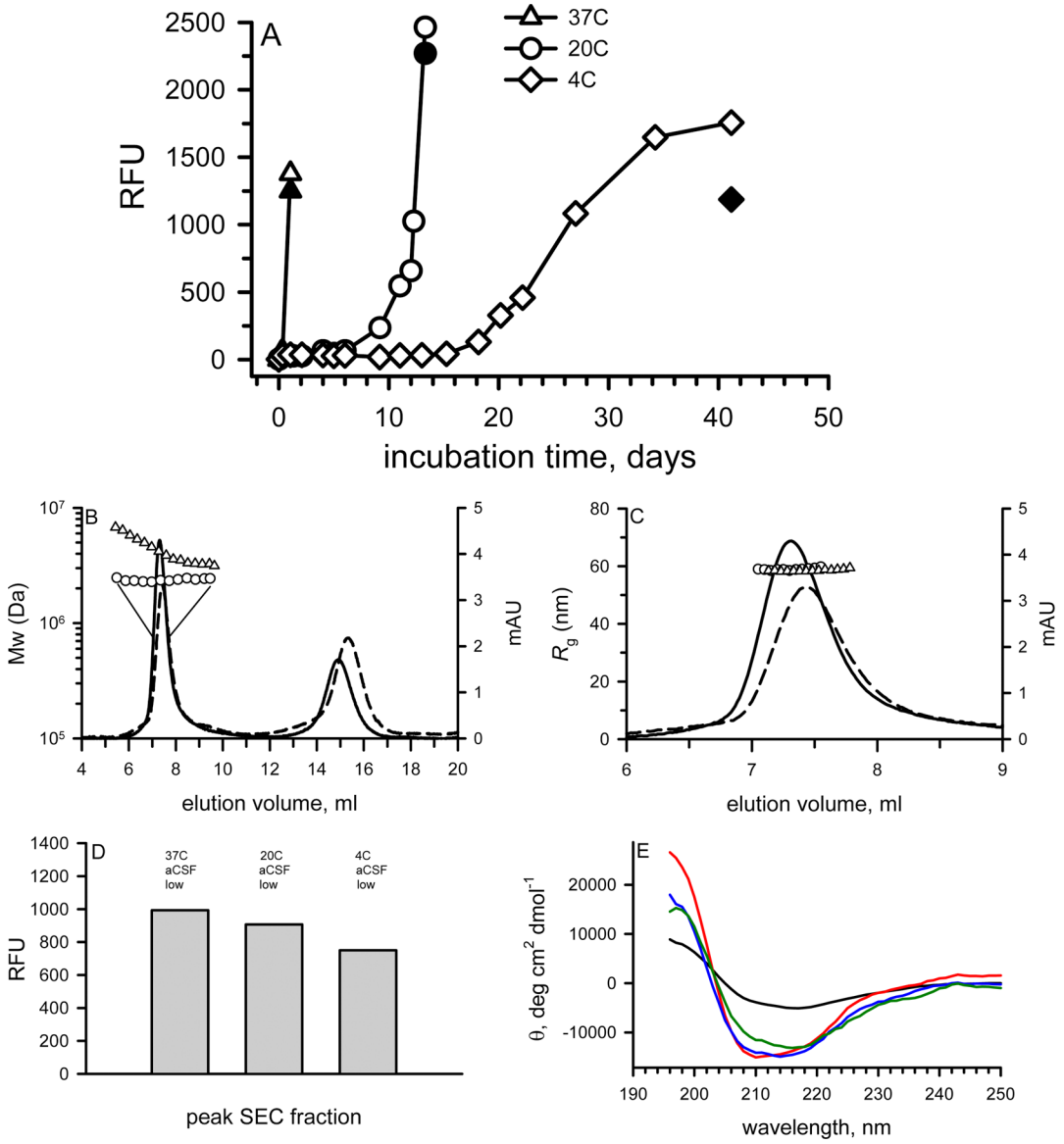

Figure 8. Aβ(1−42) aggregation is highly temperature-dependent in aCSF low NaCl, yet similar soluble species are formed. (A) Solutions of SEC-purified Aβ(1−42) monomers (40 μM) in aCSF low NaCl were incubated at 4 (△), 20 (○), and 37 °C (◇). ThT fluorescence measurements were taken at periodic times. At the final aggregation time points for each temperature, the solutions were centrifuged at 18000*g* for 10 min, and the supernatants were probed for ThT fluorescence (filled symbols). (B and C) Centrifugation supernatants (0.5 mL) from the solutions in panel A were repurified on SEC in aCSF low NaCl. The 280 nm absorbance elution traces for the 37 °C elution are shown in Figure 7B (−−−), while the 20 (—) and 4 °C (−−−) aggregation solutions are shown above (right *y*-axis). M_w (B) and R_g (C) values (left *y*-axes) were determined in line with SEC−MALS for each 0.167 mL fraction (slice) through the void volume peaks for 20 (○) and 4 °C (△). Because the complete elution trace is shown in panel B, the M_w values, determined from the full width at half-maximum of each peak, have been expanded. (D) ThT fluorescence measurements of the peak void volume fractions eluted after SEC at 1.04 (37 °C incubation), 13.3 (20 °C incubation), and 41.2 (4 °C incubation) days were obtained. Because of the low Aβ(1−42) concentrations, samples (35 μL) were mixed in a 1:1 ratio with 10 μM ThT to enhance the fluorescence signal. (E) Peak void volume SEC fractions and the precentrifuge solution from the 37 °C aCSF reaction depicted in Figure 7A (second set of bars) (black line) were analyzed by CD. Spectra were obtained as described in Experimental Procedures for SEC-isolated peak void volume fractions from the 37 °C (red line), 20 °C (blue line), and 4 °C (green line) reactions in aCSF low NaCl. MRW was calculated on the basis of 40 μM Aβ(1−42) for 37 °C in aCSF and 7, 6, and 5 μM for 37, 20, and 4 °C aggregation reactions in aCSF low NaCl, respectively.

from 2478 to 2281 kDa (mean of 2357 kDa, 522 monomers) and from 59 to 58 nm (mean of 59 nm), respectively, for the 20 °C reaction and from 6779 to 3140 kDa (mean of 4324 kDa, 958 monomers) and from 59 to 58 nm (mean of 58 nm), respectively, for the 4 °C reaction (Figure 8B,C). Peak fractions collected from the void volume of the three SEC elutions all exhibited similar ThT fluorescence levels (Figure 8D), the only differences corresponding to the slightly different Aβ concentrations (37 °C, fraction 16, 7 μM; 20 °C, fraction 16, 6 μM; 4 °C, fraction 16, 5 μM).

Circular dichroism (CD) was utilized to further probe the secondary structure of the SEC-isolated soluble Aβ(1−42) protofilaments. The precentrifuge insoluble fibrils that were obtained after overnight incubation of SEC-purified Aβ(1−42) monomers in aCSF (described in Figure 7A) had significant amounts of β-sheet structural elements. Secondary structure estimates using CONTINLL in the CDPro software package

DOI: 10.1021/bi500957g
Biochemistry 2015, 54, 2193−2204

determined 8% helix, 63% sheet/turn, and 29% coil for the structures formed in the higher-NaCl aCSF buffer (Figure 8E). Surprisingly, the soluble Aβ(1−42) protofilaments formed in aCSF low NaCl and isolated by SEC contained significant α-helical structure along with the β-sheet (Figure 8E). The soluble species formed most rapidly at 37 °C exhibited the most helical structure (45% helix, 25% sheet/turn, and 30% coil) with the slower-forming soluble species at 20 °C (34% helix, 34% sheet/turn, and 32% coil) and 4 °C (24% helix, 54% sheet/turn, and 22% coil) containing less. The molar ellipticities were different because of the higher solution concentration of the fibrils formed in aCSF (40 μM) compared to that of the SEC-isolated protofilaments formed in aCSF low NaCl (4−7 μM).

DISCUSSION

Two of the most frequently used *in vitro* Aβ aggregate preparations for biological studies have been reported to result in the formation of either "protofibrils" or "oligomers". Aβ protofibrils were first observed more than 15 years ago and were characterized as precursors along the fibril-forming pathway.[14,39] The conditions have been optimized over time to increase protofibril yields and minimize polydispersity.[40,41] An important factor involved solvation of the Aβ under alkaline conditions using either NH_4OH or NaOH. Typically, Aβ is synthesized as a trifluoroacetic acid salt, which when solubilized results in an acidic solution. Transfer into buffers to conduct studies at neutral pH required crossing the Aβ isoelectric point (pI 5.5). The alkaline method avoided this step and significantly slowed the introduction of polydispersity and loss of solubility experienced at the pI. Because of the widespread interest in soluble Aβ species, detailed procedures for the preparation of protofibrillar Aβ have continued to be refined and reported.[28] Because many studies are aimed at investigating the biological effects of Aβ protofibrils, we have recently reported the preparation and characterization of Aβ(1−42) protofibrils in antibiotic-supplemented F-12 cell culture medium[32] and a carbonate- and phosphate-based aCSF buffer.[36]

SEC isolation of the protofibrils has allowed further structural and morphological analysis. As determined by circular dichroism (CD) and ThT binding and fluorescence, Aβ protofibrils possess significant β-structure, albeit to a lesser extent than Aβ fibrils. Microscopy analysis has shown curvilinear structures <200 nm in length. However, true M_w determination for this specific type of protofibril preparation has not been reported. In this study, we used SEC−MALS to provide the first characterization of M_w and R_g for rapidly formed Aβ(1−42) protofibrils and compare the findings with those obtained for Aβ(1−42) oligomers.

Aβ(1−42) protofibrils eluted in the void volume of a Superdex 75 column (fractionation range of 3−70 kDa), yet size separation was observed as the protofibril M_w values averaged 2119 kDa at the leading edge of the concentration peak and 307 kDa at the trailing edge (2600 kDa maximum, 208 kDa minimum) over four separate SEC−MALS analyses. The average M_w range represents an equivalent protofibril size in monomer units from 68 to 469 monomers. Protofibrils are exceedingly soluble and relatively small compared to fibrils, but they do not exist as a discrete homogeneous population. In fact, there was significant polydispersity in the protofibril size distribution. Interestingly, no species were observed between protofibrils and Aβ(1−42) monomers (4514 Da). Aβ(1−42) protofibrils are formed rapidly (0.5−2 h) after addition of aCSF to the NaOH-solubilized Aβ peptide. A much longer incubation time is necessary for the formation of Aβ(1−40) protofibrils. Rosenberry and colleagues previously used SEC−MALS to examine soluble Aβ(1−40) protofibrils prepared from the SEC-purified monomer under vigorous agitation conditions.[19,29] Protofibril sizes in the earlier study were larger (M_w = 7000−32000 kDa; R_g = 50−120 nm) than those observed in the study presented here and likely represented protofibrils at later stages in the aggregation process because of the mechanical agitation.

Our SEC−MALS analysis of the Aβ(1−42) oligomer preparation was somewhat surprising in that, in multiple preparations, oligomers were larger than protofibrils. These results are consistent with those of a previous light scattering analysis of a soluble oligomeric preparation termed an amyloid-β-derived diffusible ligands (ADDLs) oligomer preparation.[29] Hepler et al. used SEC−MALS to characterize the size of ADDLs in solution and observed a polydisperse mixture of oligomers ranging in size from nearly 1000 kDa at the leading edge of the peak to 150 kDa at the trailing edge. The method used for the preparation of ADDLs in the previous study is the basis for the oligomer preparation we characterize in this study and has been rigorously detailed in a separate report.[20] The M_w values obtained for Aβ(1−42) oligomers in our current study averaged 2379 kDa at the leading edge and 611 kDa at the trailing edge, larger than those in the earlier investigation. Two factors likely played a role in this size difference. One, we observed that oligomer formation and polymerization were more variable than protofibril formation and required multiple analyses to obtain a median size. While the oligomer solution always contained higher-M_w species, the M_w values could fluctuate 2−3-fold. Two, different Aβ dn/dc values were used in the two studies. Hepler et al. used an empirically derived value of 0.241 mL g^{-1}, while in the study presented here, the general protein value of 0.186 mL g^{-1} was incorporated. The latter value was also used in previous Aβ studies.[19] Incorporation of the higher dn/dc value would bring our oligomer M_w values closer in line with those of Hepler et al.

While Aβ(1−42) oligomers were typically larger than protofibrils in terms of M_w, R_g, and R_H, the two species showed similarities in ThT binding and fluorescence and extended conformation. However, there was a notable difference in morphology. The TEM image in Figure 6 showing the spherical globular morphology of an SEC-isolated oligomer preparation is similar to that observed previously by AFM.[20,29] Morphologically, it is not clear why Aβ oligomers are consistently characterized as globular spheroid by microscopy yet in solution are observed as higher-molecular weight aggregates with an extended conformation. Oligomeric Aβ has typically been characterized by denaturing (SDS) or nondenaturing (native) gel electrophoresis with a focus on dimeric, trimeric, tetrameric, and other low-molecular weight species.[18,20,42] However, significant amounts of these small oligomers were not detected by SEC−MALS between the higher-molecular weight species and the monomers, including the leading edge of the monomer peak. There is a possibility that these small oligomeric Aβ species exist at very low levels and are difficult to detect in solution. One conclusion of this study is that, in most conventional preparations starting with dry Aβ(1−42) peptide, both protofibrils and oligomers may coexist and possess size and structural similarities. However, one area of divergence may be solvent-exposed aggregate surfaces. This difference would likely alter the surface properties

DOI: 10.1021/bi500957g
Biochemistry 2015, 54, 2193−2204

of each species, greatly impact adsorption to various substrates, and lead to divergent apparent morphologies using microscopy. This is consistent with the many observations that Aβ aggregates typically have some degree of structural polydispersity and are rarely homogeneous.

One of the concerns in the studies of aggregation-prone peptides and/or proteins is the starting material. Routinely used preparations involve reconstitution from a dry peptide at high concentrations. Even though precautions are typically taken such as HFIP pretreatment and high-alkaline reconstitution, some preexisting aggregate formation may be possible during synthesis, dissolution, lyophilization, drying, and storage of the Aβ(1−42) stocks. These aggregates may persist even after HFIP or DMSO treatment. Our studies indicate that Aβ(1−42) protofibril formation is rapid and favorable at high concentrations. However, at lower concentrations and after further purification of Aβ(1−42) monomers by SEC, the lag phase prior to nucleation was extended. Once nucleation had occurred, the aggregation progressed quickly to long slender soluble protofilaments at lower ionic strengths. These species rapidly achieved M_w and R_g values of 3000 kDa (665 monomers) and 60 nm, respectively. A higher ionic strength favored high-mass, insoluble fibril formation, which hindered some solution analyses. Interestingly, no globular or spherical oligomeric species were observed in the aggregation reaction mixtures that started with SEC-purified Aβ(1−42) monomers. These species may be present prior to the onset of ThT binding and fluorescence.

The experimental R_g/R_H ratio can provide conformational information about polymeric species. R_g/R_H values of 0.78 for spheres (globular proteins) and 1.30 for flexible Gaussian chains are typical.[43] Both Aβ(1−42) protofibrils and oligomers had R_g/R_H ratios of >0.78 indicative of an extended conformation. The average R_g/R_H value obtained over multiple separate experiments was 1.08 ± 0.30 (standard deviation) for protofibrils and 1.19 ± 0.22 for oligomers. The standard deviation provided evidence of some conformational polydispersity in both preparations and may represent the presence of alternate structures. A more detailed analysis of fractional R_g/R_H through each protofibril and oligomer peak yielded values of 1.09 ± 0.31 (standard deviation) and 1.11 ± 0.16 for protofibrils and oligomers, respectively. R_g/R_H comparisons were more difficult with protofilaments formed from SEC-purified Aβ(1−42) monomers because of polydispersity in the R_H measurements.

Aβ protofibrils and oligomers have been shown to elicit biological responses, including a proinflammatory response in immune cells.[32,44−48] The absolute molecular details of soluble Aβ aggregates such as protofibrils and oligomers that render them neurotoxic or proinflammatory remain to be determined. These properties will likely include size, secondary structure, overall conformation, and specific exposed surfaces. *In vitro* studies, so valuable for elucidating these fine details, will ultimately need to be validated *in vivo*.

CONCLUSION

This study is the first direct comparison of the biophysical properties of Aβ(1−42) protofibrils and oligomers using their respective conventional preparations. These two species are part of a broader class of soluble aggregated Aβ assemblies believed to play a critical role in AD pathogenesis. Although they are very soluble, we found that both species exist as higher-molecular weight aggregates in solution, with the oligomers actually being larger than the protofibrils. There were notable biophysical similarities and key morphological differences between the two, both of which differed from soluble protofilaments formed from SEC-isolated monomers. This study provides important information about the biophysical properties of Aβ, and this knowledge will support future studies aimed at understanding how the properties contribute to the neurodegeneration in AD.

AUTHOR INFORMATION

Corresponding Author

*Department of Chemistry and Biochemistry, University of Missouri—St. Louis, One University Boulevard, St. Louis, MO 63121. E-mail: nicholsmic@umsl.edu. Telephone: (314) 516-7345. Fax: (314) 516-5342.

Funding

This work was supported by National Institute on Aging Grant R15AG033913 (M.R.N.).

Notes

The authors declare no competing financial interest.

ACKNOWLEDGMENTS

We thank the Microscopy Image and Spectroscopy Technology Laboratory in the Center for Nanoscience at the University of Missouri—St. Louis for TEM imaging.

ABBREVIATIONS

AD, Alzheimer's disease; Aβ, amyloid-β protein; aCSF, artificial cerebrospinal fluid; BSA, bovine serum albumin; GuHCl, guanidine hydrochloride; HFIP, hexafluoroisopropanol; SEC, size-exclusion chromatography; ThT, thioflavin T; Tris, tris(hydroxymethyl)aminomethane.

REFERENCES

(1) Masters, C. L., and Selkoe, D. J. (2012) Biochemistry of amyloid β-protein and amyloid deposits in Alzheimer disease. *Cold Spring Harbor Perspect. Med. 2*, a006262.

(2) Glenner, G. G., and Wong, C. W. (1984) Alzheimer's disease: Initial report of the purification and characterization of a novel cerebrovascular amyloid protein. *Biochem. Biophys. Res. Commun. 120*, 885−890.

(3) Suzuki, N., Cheung, T. T., Cai, X. D., Odaka, A., Otvos, L., Jr., Eckman, C., Golde, T. E., and Younkin, S. G. (1994) An increased percentage of long amyloid β protein secreted by familial amyloid β protein precursor (βAPP_{717}) mutants. *Science 264*, 1336−1340.

(4) Tanzi, R. E. (2012) The genetics of Alzheimer disease. *Cold Spring Harbor Perspect. Med. 2*, a006296.

(5) Hardy, J. (1997) Amyloid, the presenilins and Alzheimer's disease. *Trends Neurosci. 20*, 154−159.

(6) Jarrett, J. T., Berger, E. P., and Lansbury, P. T., Jr. (1993) The carboxy terminus of the β amyloid protein is critical for the seeding of amyloid formation: Implications for the pathogenesis of Alzheimer's disease. *Biochemistry 32*, 4693−4697.

(7) Gravina, S. A., Ho, L., Eckman, C. B., Long, K. E., Otvos, L., Jr., Younkin, L. H., Suzuki, N., and Younkin, S. G. (1995) Amyloid β protein (Aβ) in Alzheimer's disease brain. Biochemical and immunocytochemical analysis with antibodies specific for forms ending at Aβ40 or Aβ42(43). *J. Biol. Chem. 270*, 7013−7016.

(8) Bitan, G., Kirkitadze, M. D., Lomakin, A., Vollers, S. S., Benedek, G. B., and Teplow, D. B. (2003) Amyloid β-protein (Aβ) assembly: Aβ40 and Aβ42 oligomerize through distinct pathways. *Proc. Natl. Acad. Sci. U.S.A. 100*, 330−335.

(9) Findeis, M. A. (2007) The role of amyloid β peptide 42 in Alzheimer's disease. *Pharmacol. Ther. 116*, 266−286.

DOI: 10.1021/bi500957g
Biochemistry 2015, 54, 2193−2204

(10) Tarawneh, R., and Holtzman, D. M. (2010) Biomarkers in translational research of Alzheimer's disease. *Neuropharmacology 59*, 310−322.
(11) Kayed, R., Head, E., Thompson, J. L., McIntire, T. M., Milton, S. C., Cotman, C. W., and Glabe, C. G. (2003) Common structure of soluble amyloid oligomers implies common mechanism of pathogenesis. *Science 300*, 486−489.
(12) Mittag, J. J., Milani, S., Walsh, D. M., Radler, J. O., and McManus, J. J. (2014) Simultaneous measurement of a range of particle sizes during $A\beta_{1-42}$ fibrillogenesis quantified using fluorescence correlation spectroscopy. *Biochem. Biophys. Res. Commun. 448*, 195−199.
(13) Harper, J. D., Wong, S. S., Lieber, C. M., and Lansbury, P. T., Jr. (1999) Assembly of Aβ amyloid peptides: An *in vitro* model for a possible early event in Alzheimer's disease. *Biochemistry 38*, 8972−8980.
(14) Walsh, D. M., Lomakin, A., Benedek, G. B., Condron, M. M., and Teplow, D. B. (1997) Amyloid β-protein fibrillogenesis: Detection of a protofibrillar intermediate. *J. Biol. Chem. 272*, 22364−22372.
(15) Walsh, D. M., Hartley, D. M., Kusumoto, Y., Fezoui, Y., Condron, M. M., Lomakin, A., Benedek, G. B., Selkoe, D. J., and Teplow, D. B. (1999) Amyloid β-protein fibrillogenesis: Structure and biological activity of protofibrillar intermediates. *J. Biol. Chem. 274*, 25945−25952.
(16) Harper, J. D., Lieber, C. M., and Lansbury, P. T., Jr. (1997) Atomic force microscopic imaging of seeded fibril formation and fibril branching by the Alzheimer's disease amyloid-β protein. *Chem. Biol. 4*, 951−959.
(17) Jarrett, J. T., and Lansbury, P. T., Jr. (1993) Seeding "one-dimensional crystallization" of amyloid: A pathogenic mechanism in Alzheimer's disease and scrapie? *Cell 73*, 1055−1058.
(18) Lambert, M. P., Barlow, A. K., Chromy, B. A., Edwards, C., Freed, R., Liosatos, M., Morgan, T. E., Rozovsky, I., Trommer, B., Viola, K. L., Wals, P., Zhang, C., Finch, C. E., Drafft, G. A., and Klein, W. L. (1998) Diffusible, nonfibrillar ligands derived from $A\beta_{1-42}$ are potent central nervous system neurotoxins. *Proc. Natl. Acad. Sci. U.S.A. 95*, 6448−6453.
(19) Nichols, M. R., Moss, M. A., Reed, D. K., Lin, W. L., Mukhopadhyay, R., Hoh, J. H., and Rosenberry, T. L. (2002) Growth of β-amyloid(1−40) protofibrils by monomer elongation and lateral association. Characterization of distinct products by light scattering and atomic force microscopy. *Biochemistry 41*, 6115−6127.
(20) Stine, W. B. J., Dahlgren, K. N., Krafft, G. A., and LaDu, M. J. (2003) *In vitro* characterization of conditions for amyloid-β peptide oligomerization and fibrillogenesis. *J. Biol. Chem. 278*, 11612−11622.
(21) Cohen, S. I., Linse, S., Luheshi, L. M., Hellstrand, E., White, D. A., Rajah, L., Otzen, D. E., Vendruscolo, M., Dobson, C. M., and Knowles, T. P. (2013) Proliferation of amyloid-β42 aggregates occurs through a secondary nucleation mechanism. *Proc. Natl. Acad. Sci. U.S.A. 110*, 9758−9763.
(22) Haass, C., and Selkoe, D. J. (2007) Soluble protein oligomers in neurodegeneration: Lessons from the Alzheimer's amyloid β-peptide. *Nat. Rev. Mol. Cell Biol. 8*, 101−112.
(23) Walsh, D. M., and Selkoe, D. J. (2007) Aβ oligomers: A decade of discovery. *J. Neurochem. 101*, 1172−1184.
(24) Chromy, B. A., Nowak, R. J., Lambert, M. P., Viola, K. L., Chang, L., Velasco, P. T., Jones, B. W., Fernandez, S. J., Lacor, P. N., Horowitz, P., Finch, C. E., Krafft, G. A., and Klein, W. L. (2003) Self-assembly of Aβ(1−42) into globular neurotoxins. *Biochemistry 42*, 12749−12760.
(25) Deshpande, A., Mina, E., Glabe, C., and Busciglio, J. (2006) Different conformations of amyloid β induce neurotoxicity by distinct mechanisms in human cortical neurons. *J. Neurosci. 26*, 6011−6018.
(26) Hartley, D. M., Walsh, D. M., Ye, C. P., Diehl, T., Vasquez, S., Vassilev, P. M., Teplow, D. B., and Selkoe, D. J. (1999) Protofibrillar intermediates of amyloid β-protein induce acute electrophysiological changes and progressive neurotoxicity in cortical neurons. *J. Neurosci. 19*, 8876−8884.
(27) Ye, C. P., Selkoe, D. J., and Hartley, D. M. (2003) Protofibrils of amyloid β-protein inhibit specific K^+ currents in neocortical cultures. *Neurobiol. Dis. 13*, 177−190.
(28) Jan, A., Hartley, D. M., and Lashuel, H. A. (2010) Preparation and characterization of toxic Aβ aggregates for structural and functional studies in Alzheimer's disease research. *Nat. Protoc. 5*, 1186−1209.
(29) Hepler, R. W., Grimm, K. M., Nahas, D. D., Breese, R., Dodson, E. C., Acton, P., Keller, P. M., Yeager, M., Wang, H., Shughrue, P., Kinney, G., and Joyce, J. G. (2006) Solution state characterization of amyloid β-derived diffusible ligands. *Biochemistry 45*, 15157−15167.
(30) Silveira, J. R., Raymond, G. J., Hughson, A. G., Race, R. E., Sim, V. L., Hayes, S. F., and Caughey, B. (2005) The most infectious prion protein particles. *Nature 437*, 257−261.
(31) Bhak, G., Lee, J. H., Hahn, J. S., and Paik, S. R. (2009) Granular assembly of α-synuclein leading to the accelerated amyloid fibril formation with shear stress. *PLoS One 4*, e4177.
(32) Paranjape, G. S., Gouwens, L. K., Osborn, D. C., and Nichols, M. R. (2012) Isolated amyloid-β(1−42) protofibrils, but not isolated fibrils, are robust stimulators of microglia. *ACS Chem. Neurosci. 3*, 302−311.
(33) Wyatt, P. J. (1993) Light scattering and the absolute characterization of macromolecules. *Anal. Chim. Acta 272*, 1−40.
(34) Tanford, C. (1961) *Physical chemistry of macromolecules*, John Wiley and Sons, Inc., New York.
(35) Sreerama, N., and Woody, R. W. (2000) Estimation of protein secondary structure from circular dichroism spectra: Comparison of CONTIN, SELCON, and CDSSTR methods with an expanded reference set. *Anal. Biochem. 287*, 252−260.
(36) Paranjape, G. S., Terrill, S. E., Gouwens, L. K., Ruck, B. M., and Nichols, M. R. (2013) Amyloid-(1−42) protofibrils formed in modified artificial cerebrospinal fluid bind and activate microglia. *J. Neuroimmune Pharmacol. 8*, 312−322.
(37) LeVine, H. (1993) Thioflavine T interaction with synthetic Alzheimer's disease β-amyloid peptides: Detection of amyloid aggregation in solution. *Protein Sci. 2*, 404−410.
(38) Kheterpal, I., Lashuel, H. A., Hartley, D. M., Walz, T., Lansbury, P. T., Jr., and Wetzel, R. (2003) Aβ protofibrils possess a stable core structure resistant to hydrogen exchange. *Biochemistry 42*, 14092−14098.
(39) Harper, J. D., Wong, S. S., Lieber, C. M., and Lansbury, P. T., Jr. (1997) Observation of metastable Aβ amyloid protofibrils by atomic force microscopy. *Chem. Biol. 4*, 119−125.
(40) Fezoui, Y., Hartley, D. M., Harper, J. D., Khurana, R., Walsh, D. M., Condron, M. M., Selkoe, D. J., Lansbury, P. T., Jr., Fink, A. L., and Teplow, D. B. (2000) An improved method of preparing the amyloid β-protein for fibrillogenesis and neurotoxicity experiments. *Amyloid 7*, 166−178.
(41) Teplow, D. B. (2006) Preparation of amyloid β-protein for structural and functional studies. *Methods Enzymol. 413*, 20−33.
(42) Ferrera, D., Mazzaro, N., Canale, C., and Gasparini, L. (2014) Resting microglia react to Aβ42 fibrils but do not detect oligomers or oligomer-induced neuronal damage. *Neurobiol. Aging 35*, 2444−2457.
(43) Rubinstein, M., and Colby, R. (2003) *Polymer Physics*, Oxford University Press, Oxford, U.K.
(44) Ajit, D., Udan, M. L., Paranjape, G., and Nichols, M. R. (2009) Amyloid-β(1−42) fibrillar precursors are optimal for inducing tumor necrosis factor-α production in the THP-1 human monocytic cell line. *Biochemistry 48*, 9011−9021.
(45) Parvathy, S., Rajadas, J., Ryan, H., Vaziri, S., Anderson, L., and Murphy, G. M., Jr. (2009) Aβ peptide conformation determines uptake and interleukin-1α expression by primary microglial cells. *Neurobiol. Aging 30*, 1792−1804.
(46) Floden, A. M., and Combs, C. K. (2006) β-Amyloid stimulates murine postnatal and adult microglia cultures in a unique manner. *J. Neurosci. 26*, 4644−4648.
(47) White, J. A., Manelli, A. M., Holmberg, K. H., Van Eldik, L. J., and Ladu, M. J. (2005) Differential effects of oligomeric and fibrillar

DOI: 10.1021/bi500957g
Biochemistry 2015, 54, 2193−2204

amyloid-β1−42 on astrocyte-mediated inflammation. *Neurobiol. Dis. 18*, 459−465.
(48) Heurtaux, T., Michelucci, A., Losciuto, S., Gallotti, C., Felten, P., Dorban, G., Grandbarbe, L., Morga, E., and Heuschling, P. (2010) Microglial activation depends on β-amyloid conformation: Role of the formylpeptide receptor 2. *J. Neurochem. 114*, 576−586.

DOI: 10.1021/bi500957g
Biochemistry 2015, 54, 2193−2204